of positive and negative cooperativity between the tRNA and the small substrates as well as to inhibition or activation of the kinetics of adenylate synthesis. They are almost certainly involved in as yet unrecognized mechanisms of half-of-the-sites mechanisms (Jakes & Fersht, 1975; Fasiolo et al., 1977). The results presented here confirm and extend previous conclusions by von der Haar & Gaertner (1975) on the role of the tRNA amino acid acceptor end in aminoacylation kinetics.

References

Baltzinger, M., & Remy, P. (1977) *FEBS Lett. 79*, 177–120.

Baltzinger, M., Fasiolo, F., & Remy, P. (1979) *Eur. J. Biochem. 97*, 481–494.

Berther, J. M., Meyer, P., & Dutler, H. (1974) *Eur. J. Biochem. 47*, 151–163.

Deutscher, M. P. (1967) *J. Biol. Chem. 242*, 1132–1139.

Eadie, G. S. (1942) *J. Biol. Chem. 146*, 85–93.

Ehrlich, R., Lefevre, J. F., & Remy, P. (1980) *Eur. J. Biochem. 103*, 145–153.

Fasiolo, F., & Ebel, J.-P. (1974) *Eur. J. Biochem. 49*, 257–263.

Fasiolo, F., & Fersht, A. R. (1978) *Eur. J. Biochem. 85*, 85–88.

Fasiolo, F., Befort, N., Boulanger, Y., & Ebel, J.-P. (1970) *Biochim. Biophys. Acta 217*, 305–318.

Fasiolo, F., Remy, P., Pouyet, J., & Ebel, J.-P. (1974) *Eur. J. Biochem. 50*, 227–236.

Fasiolo, F., Ebel, J.-P., & Lazdunski, M. (1977) *Eur. J. Biochem. 73*, 7–15.

Fersht, A. R., Gangloff, J., & Dirheimer, G. (1978) *Biochemistry 17*, 3740–3746.

Holler, E. (1978) *Angew. Chem., Int. Ed. Engl. 17*, 648–656.

Jacques, Y., & Blanquet, S. (1977) *Eur. J. Biochem. 79*, 433–441.

Jakes, R., & Fersht, A. R. (1975) *Biochemistry 14*, 3344–3350.

Kern, D., Potier, S., Boulanger, Y., & Lapointe, J. (1979) *J. Biol. Chem. 254*, 518–524.

Khym, J. X., & Uziel, M. (1968) *Biochemistry 7*, 422–426.

Krauss, G., von der Haar, F., & Maass, G. (1979) *Biochemistry 18*, 4755–4761.

Lefevre, J.-F., Ehrlich, R., & Remy, P. (1980) *Eur. J. Biochem. 103*, 155–159.

Mitra, S. K., & Mehler, A. H. (1967) *J. Biol. Chem. 242*, 5490–5499.

Pilz, I., Goral, K., & von der Haar, F. (1979) *Z. Naturforsch. C: Biosci. 34C*, 20–26.

Pimmer, J., & Holler, E. (1979) *Biochemistry 18*, 3714–3723.

Santi, D. V., Danenberg, P. V., & Satterly, P. (1971) *Biochemistry 10*, 4804–4812.

Schmidt, J., Wang, R., Stanfield, S., & Reid, B. R. (1971) *Biochemistry 10*, 3264–3268.

von der Haar, F., & Gaertner, E. (1975) *Proc. Natl. Acad. Sci. U.S.A. 72*, 1378–1382.

Tropomyosin Stability: Assignment of Thermally Induced Conformational Transitions to Separate Regions of the Molecule†

David L. Williams, Jr., and Charles A. Swenson*

ABSTRACT: Tropomyosin was prepared from rabbit skeletal muscle and studied in a differential scanning calorimeter. The characteristics of the observed endotherms were studied as a function of pH, salt concentration, oxidation state of Cys-190, and concentration of the divalent metal ions Ca^{2+} and Mg^{2+}. The large shifts observed for the T_m values of the components of the endotherms with changing pH and salt concentration are consistent with electrostatic effects being an important determinant of the structural stability of tropomyosin. For reduced tropomyosin or tropomyosin blocked with *N*-ethylmaleimide, two endotherms were observed with T_m values of 41.5 and 52.5 °C at neutral pH in a low-salt buffer. For tropomyosin containing a disulfide link at Cys-190, two endotherms were observed with T_m values of 32 and 52 °C under the same conditions. The endotherm at 52 °C contains contributions from conformational transitions in two independent structural regions. An analysis of the heat-capacity profiles for the two large cyanogen bromide peptides, CN1A and CN1B, enabled the assignment of two components of the endotherms to structural transitions in the C-terminal region which includes Cys-190 and in the N-terminal region. Calcium and magnesium ions in the 1–10 mM range increased the stability of several of the regions of the structure, presumably by binding to localized areas of excess negative charge. Unfolding of tropomyosin in the 20–70 °C range is a multistep process and occurs with an average enthalpy of 4 cal g^{-1}.

The calcium-activated switch of skeletal muscle functions through induced conformational changes which act as signals modulating the interactions between the constituent molecules. Calcium binding to troponin causes a conformational signal to be conveyed to tropomyosin. By alteration of its interaction with actin, tropomyosin allows actin–myosin interaction and tension generation. Although there is some controversy concerning the exact molecular mechanism of calcium activation in skeletal muscle, it is clear that tropomyosin is central to the transmission of the signal initiated by the binding of calcium to troponin. Thus, some knowledge of the conformational states available to tropomyosin should assist us in determining how the intrinsic properties of this structure dictate its function in the calcium switch.

Tropomyosin is an α-helical coiled-coil protein with two identical ($\alpha\alpha$) or very closely related ($\alpha\beta$) subunits of known sequence, each consisting of 284 amino acid residues (Sodek et al., 1978; Stone & Smillie, 1978; Mak et al., 1979). In rabbit skeletal muscle, the ratio of α to β subunits is ~3.5:1 while cardiac muscle contains only the α subunit. The α-

† From the Department of Biochemistry, University of Iowa, Iowa City, Iowa 52242. *Received August 20, 1980.* This work was supported by Grant HL14388 from the National Institutes of Health.

0006-2960/81/0420-3856$01.25/0

helical chains are parallel and in register and may be covalently linked by a disulfide bond at Cys-190 (Lehrer, 1975; Johnson & Smillie, 1975). Regularities in the sequence assign each residue to a specific position, a–g, of a repeating heptet and are crucial for stability (McLachlan & Stewart, 1975).

The conformational stability of tropomyosin has been investigated with temperature and chaotropic agents as variables for perturbing its structure. It was found that rabbit skeletal muscle tropomyosin does not follow a two-state model for unfolding under reducing conditions (Woods, 1969). Investigations of tropomyosin from a variety of muscle types, including invertebrate muscle, showed that more than one step is involved in unfolding (Woods, 1976). Fluorescent spectral studies with Cys-190 oxidized [by air and with 5,5′-dithiobis(2-nitrobenzoate)], reduced, or blocked with iodoacetamide showed that the stability of tropomyosin (TM)[1] is dependent on the state of oxidation (Lehrer, 1978). Specifically, Lehrer observed a small transition in the 30–45 °C range which he suggested could be related to an inherent instability in the region of the disulfide link at Cys-190. This transition was not observed for reduced TM. Also, the T_m of the major transition of tropomyosin was decreased 7 °C when the disulfide link was cleaved. Pato & Smillie (1978) noted a marked difference in the stability of the two major fragments of TM derived from the NH_2-terminal and COOH-terminal portions of the molecule under reducing conditions. These data strongly suggest that the unfolding of the TM molecule occurs in definite regions which are perturbed by the state of oxidation.

Differential scanning calorimetry (DSC), wherein the solution heat capacity is measured as a function of temperature, is an extremely useful technique for observing and measuring the properties of thermally induced conformational transitions in macromolecules. The inherent advantage of this technique over other methods is that it measures the derivative of the progress curve; thus, small or multiple transitions in a complex envelope are more readily detected.

Using a highly sensitive calorimeter, we have systematically investigated the conformational transitions of rabbit skeletal tropomyosin as a function of oxidation state, pH, added divalent metal ions (Ca^{2+} and Mg^{2+}), and salt concentration. At least three endotherms were observed. Two of the endotherms are assigned to conformational transitions in specific regions of the structure from a study of the two large cyanogen bromide fragments.

Materials and Methods

Tropomyosin. Tropomyosin was purified according to a modification of the methods of Greaser & Gergely (1971) and Hartshorne & Mueller (1969). New Zealand white rabbit back and leg muscle was ground, washed consecutively with 0.1 M KCl, 50 mM $NaHCO_3$, 1 mM EDTA, H_2O, and five washes of acetone (all reagents from Fisher Scientific Co.), and allowed to air-dry for 48 h. This acetone powder was either stored at −20 °C or extracted twice at either 4 °C or room temperature with 25 mM Tris-HCl, 1 M KCl, 0.1 mM $CaCl_2$, 1 mM DTT, and 0.02% NaN_3 at pH 8.0. An ammonium sulfate fractionation was performed at a protein concentration of ~2 mg/mL. Solid ammonium sulfate was used for this step, and the precipitate from the 40–60% saturated fraction was resuspended in and dialyzed vs. 5 mM Tris-HCl, 0.1 mM $CaCl_2$, 0.1 mM DTT, and 0.02% NaN_3 at pH 7.5. Solid KCl was added to the viscous, turbid, and dialyzed protein solution to 1 M, and the solution was centrifuged at 10000*g* for 60 min. Two isoelectric fractionations to pH 4.6 were performed on the supernatant. Under these conditions, the tropomyosin–troponin interaction is weak, and the tropomyosin aggregates, while troponin largely stays in solution. Finally, tropomyosin was obtained from the 50–60% saturated ammonium sulfate fraction. The translucent precipitate was dialyzed vs. water for subsequent lyophilization or vs. 10 mM Tris-HCl, 1 M KCl, and 1 mM EDTA at pH 7.0 for procedures involving adjustment of the Cys-190 oxidation state.

The ability of TM to function as a component of the calcium switch was assayed according to a modification of the method of Spudich & Watt (1971). The solvent was 10 mM imidazole buffer at pH 7.0 which contained 30 mM KCl. Protein concentrations in the mixture were 0.2 mg/mL actin, 0.19 mg/mL troponin, 0.09 mg/mL tropomyosin, and 0.5 mg/mL HMM. Also present were 2 mM ATP, 5 mM $MgCl_2$, and 1 mM EDTA or 0.1 mM $CaCl_2$. The stoichiometry of the proteins in the mixture was 2:1:3.5 for TN, TM, and actin, respectively, which corresponds to a 2-fold excess of TN over TM and a 2-fold excess of TM over actin. Actin was present in a 3-fold molar excess over HMM. Addition of HMM to the solution containing actin, ATP, TN, and TM, mixed in this order, initiated the reaction. Typically, the acto-HMM ATPase activity was inhibited 45% by the addition of TM and was insensitive to the presence of calcium. The activity was decreased to 10% when troponin was added, and this inhibition was relieved by the addition of calcium.

Cross-Linked Tropomyosin. Cross-linked tropomyosin (XLTM) was made according to the method of Lehrer (1975). Briefly, this involved reducing the cysteine residues with DTT and treating them with 6 mM 5,5′-dithiobis(2-nitrobenzoic acid) (DTNB), which reacts with the free sulfhydryls and then causes disulfide linkage formation with other nearby sulfhydryls. A 40-fold excess of DTNB was used. We modified Lehrer's procedure to use NEM rather than iodoacetamide to stop the reaction. The reaction product was analyzed by $NaDodSO_4$–polyacrylamide gel electrophoresis and the percent of un-cross-linked TM obtained by densitometric analysis of the gels.

Blocked Tropomyosin. Tropomyosin was reduced by 1 mM DTT under N_2 at 40–45 °C for 90 min in 10 mM Tris-HCl, 1 M KCl, and 1 mM EDTA at pH 7.0. NEM was added in the same buffer to 2.5 times the concentration of DTT present, and stirred for 30 min. The reaction was stopped by addition of DTT. The NEM-blocked tropomyosin (NEMTM) was precipitated by adjustment of the pH to 4.6. The precipitate was homogenized and dialyzed vs. an appropriate buffer for calorimetry. If the results of $NaDodSO_4$–polyacrylamide gel electrophoresis indicated that reduction and blocking were incomplete, the reaction was run a second time. Amino acid analysis of the blocked TM showed that cysteine had been converted to *S*-(2-succinyl)cysteine which was eluted preceding aspartic acid. No other modified amino acids were detected. Since the color values of cysteine and its derivative are small, we also measured the free sulfhydryl content in $NaDodSO_4$

[1] Abbreviations used: CN1A, tropomyosin cyanogen bromide fragment residues 11–127; CN1B, tropomyosin cyanogen bromide fragment residues 142–281; DSC, heat-capacity calorimeter, differential scanning calorimetry; DTNB, 5,5′-dithiobis(2-nitrobenzoic acid); DTT, dithiothreitol; EDTA, ethylenediaminetetraacetic acid; HMM, heavy meromyosin subfragments of myosin; NEM, *N*-ethylmaleimide; NEMTM, tropomyosin with Cys-190 blocked with NEM; Tes, *N*-tris(hydroxymethyl)methyl-2-aminoethanesulfonic acid; Pipes, piperazine-*N*,*N*′-bis(2-ethanesulfonic acid); Tris, tris(hydroxymethyl)aminomethane; TM, tropomyosin; TN, troponin; XLTM, tropomyosin with Cys-190 disulfide bridges intact; $NaDodSO_4$, sodium dodecyl sulfate.

by the method of Fernandez Diez et al. (1964). Typically, about 3% of the cysteine residues were not modified by NEM.

Cyanogen Bromide Fragments. Cyanogen bromide cleavage of tropomyosin was performed according to the method of Hodges et al. (1973). Lyophilized tropomyosin was dissolved in 70% formic acid to give a protein concentration of 10 mg/mL and treated with a 100-fold excess of CNBr (relative to methionine) for 36 h at room temperature. The solution was then diluted 10× with water, frozen, and lyophilized. The lyophilized fragments were dissolved in 10 mM Tris, 2 M urea, and 0.02% NaN_3, pH 8.0, and the urea was removed by dialysis vs. 10 mM Tris and 0.02% NaN_3 at the same pH. The mixed fragment sample was applied to a Dowex 1-X2 Cl^- column equilibrated with the same buffer and eluted with a 1-L KCl gradient, 0–1 M KCl. Fractions were analyzed by $NaDodSO_4$–polyacrylamide gel electrophoresis under nonreducing conditions. Amino acid analysis was performed on the pooled fractions by using a ninhydrin absorption detection system (Beckman) or an *o*-phthalaldehyde/β-mercaptoethanol fluorescence detection system (performed in the laboratory of B. V. Plapp).

Protein Concentration. Protein concentrations were determined by the biuret method and by absorption spectroscopy with $E^{1\%}_{277} = 3.3$ for tropomyosin (Woods, 1967).

Sodium Dodecyl Sulfate–Polyacrylamide Gel Electro-

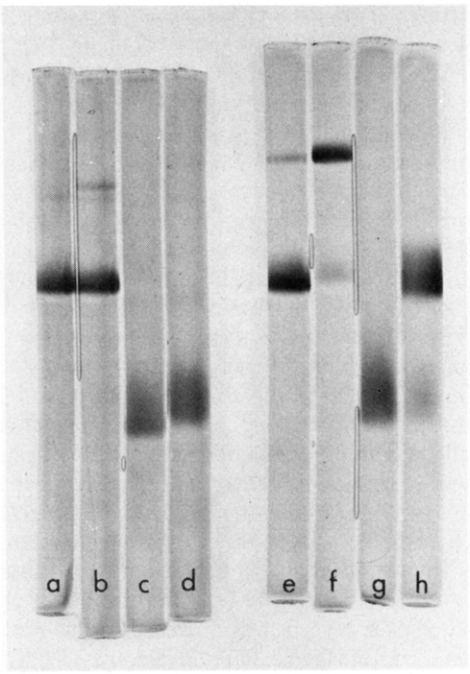

FIGURE 1: $NaDodSO_4$–polyacrylamide gel electrophoresis analysis

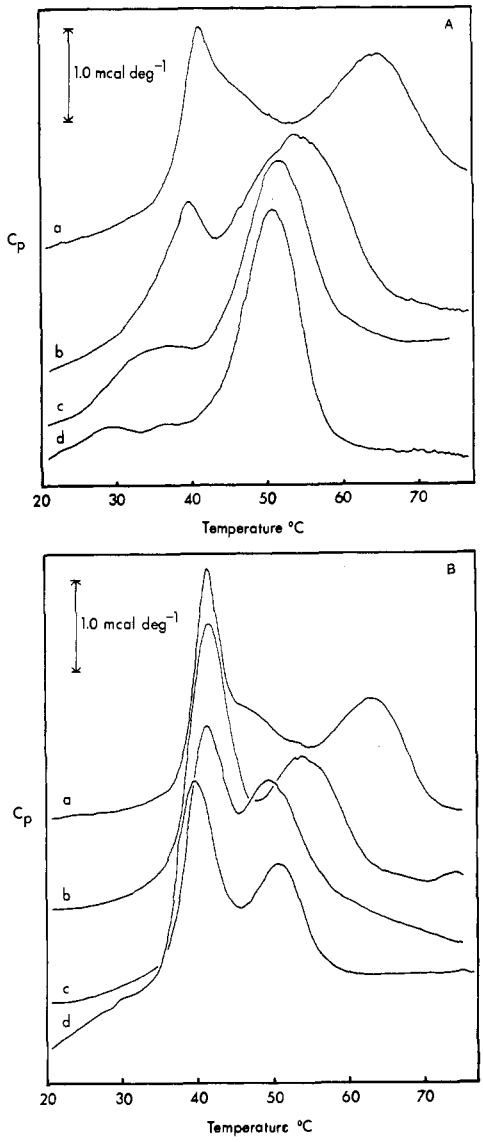

FIGURE 2: (A) Heat-capacity profiles of XLTM. Conditions: 10 mM Pipes, 100 mM KCl, 0.1 mM $MgCl_2$, and 0.02% NaN_3. (a) pH 6.0, 7.5 mg/mL protein; (b) pH 6.5, 9.2 mg/mL protein; (c) pH 7.0, 7.0 mg/mL protein; (d) pH 8.0, 8.0 mg/mL protein. Scan rate = 60 °C/h. (B) Heat-capacity profiles of NEMTM. Conditions: 10 mM Pipes, 100 mM KCl, 0.1 mM $MgCl_2$, and 0.02% NaN_3. (a) pH 6.0, 6.1 mg/mL protein; (b) pH 6.5, 7.7 mg/mL protein; (c) pH 7.0, 10.9 mg/mL protein; (d) pH 8.0, 10.1 mg/mL protein at $^2/_3$ scale. Scan rate = 60 °C/h.

transitions which have T_m values of 42 and 63 °C and an additional transition(s) with a T_m in the 45–55 °C range. At this same pH in high salt, as is shown in Figure 3, three transitions are observed for XLTM; however, asymmetry on the high-temperature side of the endotherm at 63 °C suggests that an additional transition may be present.

The heat-capacity profiles for NEMTM (Figure 2B) show two major transitions at pH 8 and 6.5 while at pH 6.0 three components are evident. Addition of ~20 mM DTT had no effect on these profiles.

The regions of the molecule in XLTM and NEMTM which correspond to the high-temperature endotherms (>45 °C) continued to increase in stability as the pH was lowered from 6 to 3, but below pH 3 their stability was decreased. The T_m values of the low-temperature endotherms continued to increase as the pH was decreased below the isoelectric point (pI = 4.6). Between pH 9 and 10, the T_m values of the low-temperature transitions decreased, indicating a decrease in the stability of the domains involved, whereas the T_m values for

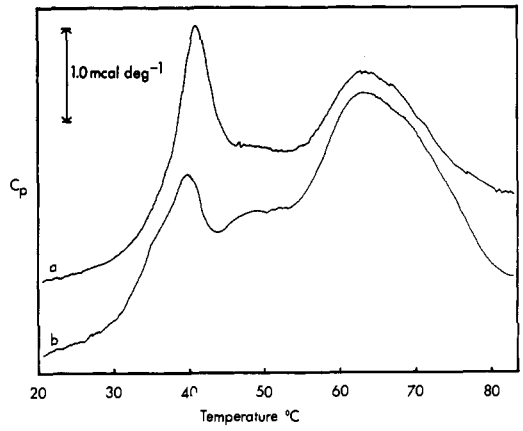

FIGURE 3: Heat-capacity profiles of NEMTM and XLTM. Conditions were 10 mM Pipes, 1 M KCl, 0.1 mM $MgCl_2$, and 0.02% NaN_3, pH 6.0. (a) [NEMTM] = 8.4 mg/mL; (b) [XLTM] = 9.9 mg/mL. Scan rate = 60 °C/h.

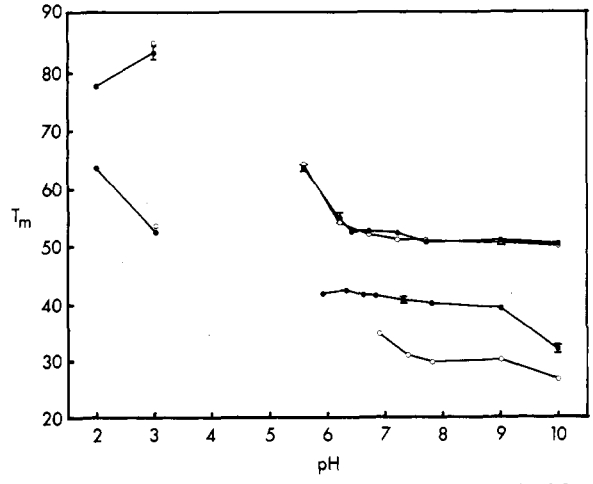

FIGURE 4: T_m values of the major endotherms of XLTM and NEMTM plotted as a function of pH. Conditions were 10 mM buffer, 100 mM KCl, 0.1 mM $MgCl_2$, and 0.02% NaN_3. The following buffers were used: malonate, pH 2–3; Pipes, pH 6–8; Tes, pH 7–8; Tris, pH 8–9; glycine, pH 9–10. The plotted pH values were obtained by correcting the measured pH at 20 °C to the value expected at the T_m with the known enthalpy of ionization. Measurements near the isoelectric pH were not taken due to difficulties with protein solubility. (○) XLTM; (●) NEMTM.

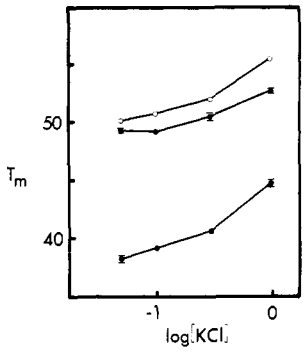

FIGURE 5: T_m values of the major endotherms of XLTM and NEMTM plotted as a function of salt concentration. Conditions were 10 mM Pipes, 0.1 mM $MgCl_2$, and 0.02% NaN_3, pH 8.0, at 50 mM, 100 mM, 300 mM, and 1 M KCl. (○) XLTM; (●) NEMTM.

the high-temperature transitions were not affected. These results are summarized in Figure 4. The plotted pH values at the transition temperatures are corrected for the enthalpies of ionization of the buffers.

The addition of neutral salt was noted to increase the T_m

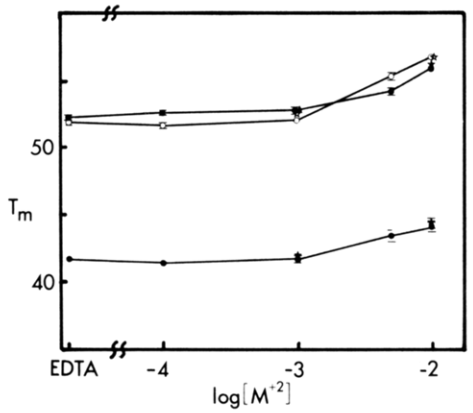

FIGURE 6: T_m values of the major endotherms of XLTM and NEMTM plotted as a function of divalent cation concentrations. Conditions were 10 mM Pipes, 100 mM KCl, and 0.02% NaN_3, pH 7.0, at 1 mM EDTA and 0.1, 1, 5, and 10 mM $MgCl_2$ or 1 and 10 mM $CaCl_2$. (○) XLTM with Mg^{2+} and EDTA; (★) XLTM with Ca^{2+}; (●) NEMTM with Mg^{2+} and EDTA; (★) NEMTM with Ca^{2+}. Lines are drawn for EDTA/Mg^{2+} samples only.

values of all the transitions. A summary of typical data at pH 8.0 is presented in Figure 5. Divalent cations, specifically Ca^{2+} and Mg^{2+}, were also noted to cause the T_m to increase. Data from these experiments at pH 7.0 are presented in Figure 6. As the concentration of Ca^{2+} or Mg^{2+} was increased from 0 (1 mM EDTA) to 1 mM, the T_m value of the major transition remained constant for XLTM and NEMTM. A further increase in concentration of divalent cation from 1 to 10 mM caused the T_m values to increase to 56.5 and 44.5 °C, respectively. All transitions in both samples were reversible with the exception of the low-temperature transition in NEMTM, which was approximately 75% reversible. The effects of aggregation were negligible since the same profiles were obtained at low and high salt (1 M), except for small shifts associated with electrostatic effects, and at protein concentrations from 1 to 15 mg/mL.

The enthalpies of the transitions were found to increase with increasing T_m. At pH 7.0, ΔH_d for the sum of the major transitions of NEMTM was 4.8 ± 0.2 cal g^{-1}. For XLTM at the same pH, ΔH_d was 4.2 ± 0.1 cal g^{-1}. The average deviations were ±9% for XLTM and ±11% for NEMTM. The largest standard deviation for ΔH_d determined under one set of conditions was ±28%; the smallest was ±1%. These errors arise primarily from uncertainty in fixing the base line and to a smaller extent from errors in measuring the protein concentration. Determination of ΔC_p for these transitions was attempted, but due to the large error it is not reported. It was, however, positive in all cases.

For location of the regions of the TM sequence which give rise to the observed endotherms, the heat-capacity profiles of the two large cyanogen bromide fragments were determined. Following the nomenclature of Hodges et al. (1973), who first prepared them, the small fragment composed of residues 11–127 is CN1A, and the larger fragment, residues 142–281, is CN1B. The separation of the fragment mixture prepared by cyanogen bromide cleavage as achieved on a Dowex 1-X2 chloride column is shown is Figure 7. In the inset is shown the analysis of selected fractions by $NaDodSO_4$–polyacrylamide gel electrophoresis under nonreducing conditions. The migration of CN1A (fractions a–d) corresponded to a molecular weight of 16 000 g mol^{-1} and is insensitive to added reducing agents. The mobility of CN1B (fractions e–i) corresponded to a molecular weight of 40 000 g mol^{-1} and under reducing conditions corresponded to a molecular weight of 19 000 g mol^{-1}. Identification of the fragments was made from the results of amino acid analysis, which agreed closely with the known sequences. This identity was substantiated by the A_{280} ratio of CN1A to CN1B, which approximates the 1:6 ratio of aromatic amino acids in the fragments. In addition, CN1A was eluted first from the ion-exchange column in agreement with its smaller number of negative charges. CN1B clearly contains two components which could arise from the cleavage of α- and β-tropomyosin. β-Tropomyosin contains

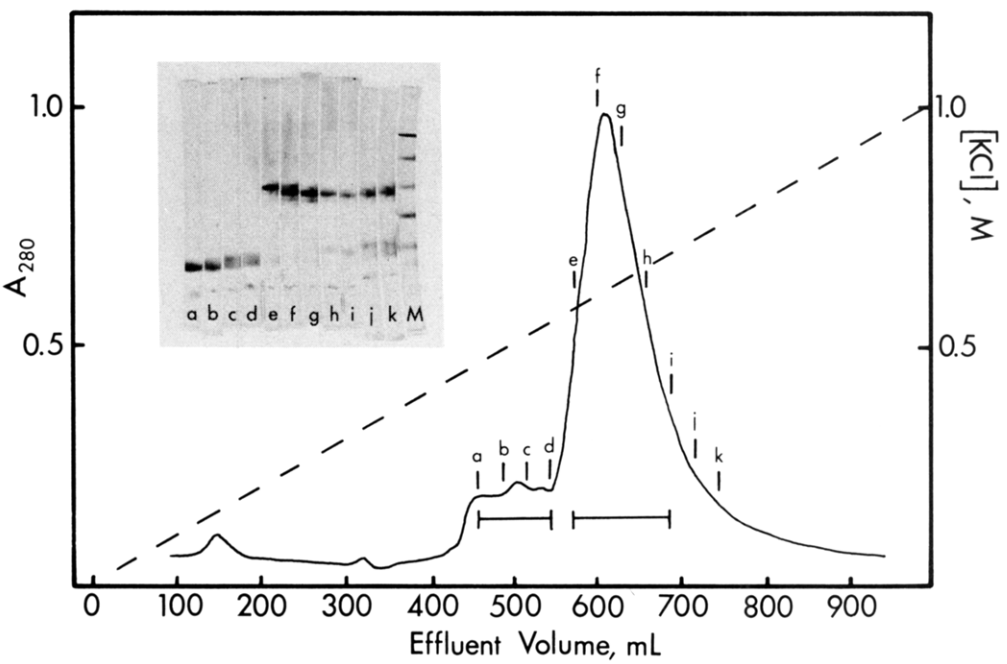

FIGURE 7: Representative elution profile from Dowex 1-X2 Cl^- chromatography of tropomyosin CNBr fragments. Sample size was 840 mg. Column volume was 140 mL. The sample was applied in 10 mM Tris and 0.02% NaN_3, pH 8.0, and after a wash was eluted with a linear 0–1 M KCl gradient (1 L) in the same buffer. The gradient indicated was estimated by volume. Inset: $NaDodSO_4$–polyacrylamide gel electrophoresis analysis was performed under nonreducing conditions. Fractions from positions a–d were pooled for CN1A, and fractions from positions e–i were pooled for CN1B. Gel M displays the pattern for marker proteins of molecular weights 94 000, 68 000, 43 000, 29 000, 20 000, and 14 000.

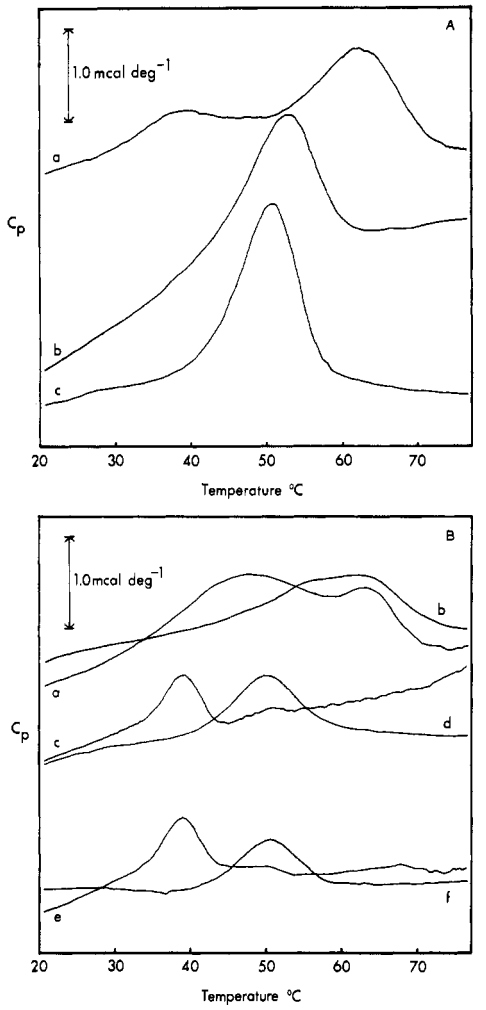

FIGURE 8: (A) Heat-capacity profiles of CN1A. Conditions were 10 mM Pipes, 100 mM KCl, 0.1 mM $MgCl_2$, and 0.02% NaN_3. (a) pH 6.0, 6.4 mg/mL protein; (b) pH 7.0, 6 mg/mL protein; (c) pH 8.0, 6.3 mg/mL protein. (B) Heat-capacity profiles of reduced and oxidized CN1B. Conditions were 10 mM Pipes, 100 mM KCl, 0.1 mM $MgCl_2$, and 0.02% NaN_3 with and without 2–5 mM DTT. (a) pH 6.0 with DTT; (b) pH 6.0 without DTT [(a) and (b) at 6.4 mg/mL protein]; (c) pH 7.0 with DTT; (d) pH 7.0 without DTT [(c) and (d) at 6 mg/mL protein]; (e) pH 8.0 with DTT; (f) pH 8.0 without DTT [(e) and (f) at 6 mg/mL protein].

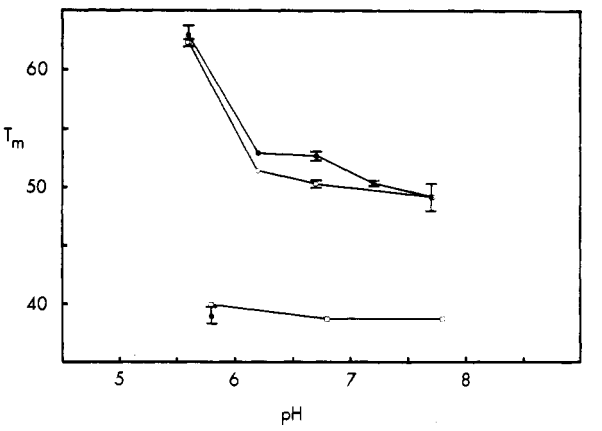

FIGURE 9: T_m values of the major endotherms of CN1A and reduced and oxidized CN1B plotted as a function of pH. Conditions were as stated in Figure 5. (●) CN1A; (○) CN1B oxidized; (□) CN1B reduced (2–5 mM DTT).

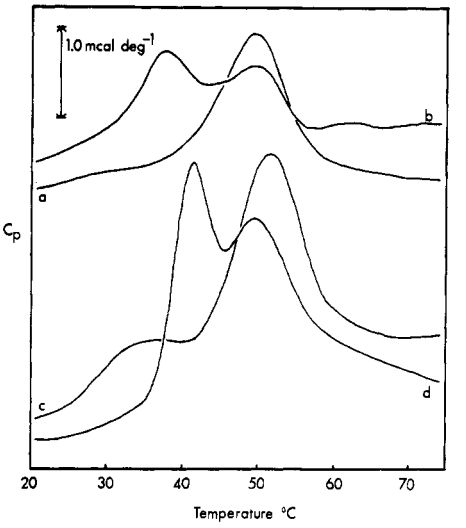

FIGURE 10: Heat-capacity profiles for mixed CNBr fragments and TM. Solvent conditions were 10 mM Pipes, pH 7.0, 100 mM KCl, 0.1 mM $MgCl_2$, and 0.02% NaN_3. (a) Mixed CN1A and CN1B (7.1 mg/mL); (b) mixed CN1A and CN1B with 20 mM DTT (7.1 mg/mL); (c) TM (6.8 mg/mL); (d) TM with 20 mM DTT (7.2 mg/mL).

additional methionines at 145 and 265 which suggests that its CN1B fragment would be smaller by approximately 2500 molecular weight units. The CN1B fragment from β-TM has less negative charge than the corresponding fragment from α-TM and thus would be expected to elute from the column ahead of the α-TM fragment. Since β-TM behaves anomalously in $NaDodSO_4$–polyacrylamide gel electrophoresis in that the molecular weight given by its mobility is too large, our suggestion is that fraction e contains the CN1B fragment of β-TM. Thus, our pooled sample (fractions e–i) is composed of CN1B fragments from α- and β-TM.

The heat-capacity profiles for CN1A and CN1B under reducing and nonreducing conditions are shown in Figure 8. The endotherms are reversible for all conditions. The profile for CN1A at pH 8.0 consists of a single endotherm at 52 °C which shows no sensitivity to added reducing agents. The small transition observed near 37 °C at pH 6.0 may be analogous to that observed between 40 and 50 °C in NEMTM. There is no evidence of this transition from measurements at pH 8.0; however, at pH 7.0, this transition could contribute to the shoulder that is apparent on the low-temperature side of the large endotherm. The pronounced slope of the heat-capacity profile at pH 7.0 was observed in two sets of duplicate measurements. We are unable to account for the large change in heat capacity with temperature for the folded form suggested by these data.

For the CN1B fragment, which includes Cys-190, the observed endotherm at pH 8.0 shifted from 50 to 39 °C upon addition of reducing agent. Similar results were obtained at pH 7.0. At pH 6.0 in the absence of reducing agents, the heat-capacity profile of CN1B contained a broad endotherm apparently consisting of two components. Addition of reducing agent caused the T_m of one broad component to decrease to 47 °C. The component that is insensitive to added reducing agent could include some oxidized TM, but this seems unlikely at a concentration of 5 mM DTT. The pH dependence of the T_m values for the transition of the fragments is summarized in Figure 9.

In Figure 10, the heat-capacity profile for an unfractionated sample (CN1A plus CN1B) is compared to the profile for TM. The two profiles are in substantial agreement except for the small decrease in the T_m value of the major transition of the fragments relative to TM. The small transition with a T_m of 32 °C observed at pH 7.0 in XLTM is also absent. In view

of the fact that 10% of the amino acids of TM are missing in the fragments, the agreement between the major transitions in TM and the fragments is excellent.

Discussion

The unfolding of the tropomyosin structure by heat is a complex process. For XLTM, the heat-capacity profiles reveal two transitions at neutral pH in low salt, a small, broad transition with a T_m of 32 °C and a large transition with a T_m of 52 °C. At pH 6.0 in 1 M KCl, the large transition has shifted to 64 °C, and it is apparent that two components are present. The data then support a minimum of three transitions and four states for XLTM in the 20–70 °C range at pH 6.0.

Two major transitions with T_m values of 41.5 and 52.5 °C are observed for the unfolding of NEMTM or reduced TM at neutral pH in low-salt buffer. The shift of a transition from 52 °C in XLTM to 41.5 °C in NEMTM suggests that the transition in NEMTM at 41.5 °C is in a domain which includes Cys-190. The transition at 52.5 °C in NEMTM is the unfolding of a region that is unaffected by the unfolding of the region which includes Cys-190. It is apparent that these two structural regions have about the same stability in XLTM. The small endotherm at 32 °C in XLTM is apparently not present in NEMTM; however, it could be masked by the large endotherm at 41.5 °C. At pH 6.0, three endotherms are observed in NEMTM with T_m values of 41.5, ~47, and 63.5 °C. The endotherms at 41.5 and 63.5 °C are simply the pH-shifted endotherms observed at pH 7.0; however, the endotherm at ~47 °C is a new feature. The endotherm at 63.5 °C is broad, and measurements at high salt concentrations suggest that it may contain two transitions. Thus, for NEMTM, the data suggest a minimum of three transitions and four states in the temperature range 20–70 °C at pH 6.0.

Earlier studies of XLTM with intrinsic fluorescence, circular dichroism (Lehrer, 1978), and heat-capacity calorimetry (Krishnan et al., 1978) noted two transitions, a small pretransition with a T_m of 30–40 °C and a major transition with a T_m of 52–60 °C. Our present work is in agreement but further suggests that the major transition may contain two components. For reduced or blocked tropomyosin, a single transition with a T_m value of 45 °C was observed by these workers. The primary difference between our results and those of earlier studies on reduced or blocked tropomyosin is the observation of an additional transition, specifically the endotherm at ~50 °C. The major transitions observed by spectroscopic and calorimetric methods arise from structural changes. It is thus unclear why the higher temperature transition of blocked TM was not observed by circular dichroism. The fluorescent result may be explained if the 50 °C transition in reduced or blocked tropomyosin is localized in the N-terminal end of the molecule which contains only a single tyrosine. Our studies on the cyanogen bromide fragments suggest that this is the case. In an attempt to reconcile our results with those of Krishnan et al. (1978), we prepared a sample of iodoacetamide-blocked tropomyosin by using their procedure. Amino acid analysis showed that all the cysteine was converted to carboxymethylcysteine and that small amounts of histidine and lysine residues were also modified. The histidine modification was only a few percent of the total, and although the lysine changed, it is difficult to quantitate as carboxymethyllysine is overlapped by isoleucine in its elution from the amino acid analyzer. The heat-capacity profile for this modified sample was the same as those we observed for both the NEM-modified sample and the DTT-reduced samples. We thus cannot explain why a different calorimetric result was obtained.

Woods (1976) observed complex melting curves for tropomyosin by use of the b_0 value of the Moffit equation to determine the fraction of helix. For reduced tropomyosin at pH 7.6 in 0.2 M salt, possibly three transitions are apparent, one at ~53 °C and two (or more) overlapping transitions in the 30–45 °C range. Our results are in qualitative agreement with this earlier study.

Potekhin & Privalov (1978) measured the heat-capacity profiles of reduced and oxidized $\alpha\alpha$-tropomyosin for a single set of solvent conditions (pH 7.1, 1 M KCl). Our results on a sample of mixed $\alpha\alpha$- and $\alpha\beta$-tropomyosin are in excellent agreement with this study. A brief study of pure $\alpha\alpha$-tropomyosin isolated from rabbit cardiac muscle showed results that were substantially the same as those that were found with the mixed sample. Thus, the unfolding of tropomyosin, $\alpha\alpha$ or $\alpha\beta$, is a complex process in that several intermediate states are involved, and heterogeneity, that is, a mixture of $\alpha\alpha$ and $\alpha\beta$ forms, does not account for the complex behavior observed by optical rotation studies (Woods, 1976) or these calorimetric studies.

Edwards & Sykes (1980) have reported the results of an NMR study on $\alpha\alpha'$- and $\beta\beta'$-tropomyosin from rabbit and have interpreted the anomalous splitting of the C-2 proton resonance of His-153 in terms of conformational states in slow equilibrium. Three states were observed in an overlapping profile of His-153 resonances in the temperature range 37–55 °C. This conclusion is in excellent agreement with our observation for NEMTM of two major between-state transitions with T_m values of 41.5 and 52.5 °C at pH 7.0.

The thermally induced spectroscopic changes and the endotherms in heat-capacity calorimetry have been correlated with structural transitions in tropomyosin. However, only for the change in the oxidation state of Cys-190 has a transition been correlated with a particular region of the coiled-coil structure. In this study, data from the heat-capacity profiles for the cyanogen bromide fragments, CN1A and CN1B, enable an assignment of two of the observed transitions of tropomyosin to separate regions of the TM structure. At pH 8.0, CN1A has a single transition whose T_m has the same pH and salt dependence as the major transition at 52 °C in XLTM and NEMTM, and is unaffected by reducing agents. CN1B has a major endotherm at 50 °C which upon reduction shifts to 39 °C. Excess heat capacity was present for all CN1B samples in the temperature range 25–40 °C but was too small to be identified as a transition which could be correlated with the pretransition. It thus seems clear that at pH 8.0 four states are present for XLTM in the temperature range 20–70 °C. Two transitions, at ~50 and 52 °C, respectively, occur in the C-terminal and N-terminal portions of the molecule and give rise to a single endotherm in tropomyosin; however, at pH 6.0 and 1 M KCl, they are partially resolved. The pretransition observed in XLTM, which is thought to be a slight opening of a region of coiled-coil structure destabilized by the disulfide link, is not observed in the CN1B fragment. Thus, our data on the fragments suggest that cleavage of the molecule 55 Å from Cys-190 has either allowed the destabilized region to unfold at lower temperature and hence escape detection or, but less likely, caused it to be part of the major transition of NEMTM at 41 °C.

For NEMTM, two major transitions are observed, and, thus, three states are expected between 20 and 70 °C at pH 8.0. The transition at 41 °C clearly can be associated with the COOH-terminal portion which includes Cys-190, and the transition at 50 °C is localized to the NH_2-terminal portion of TM. At pH 6.0, the heat-capacity profiles for NEMTM

and XLTM show an additional endotherm in the 45–50 °C range. The data on the fragments suggest that this endotherm may rise in CN1A or CN1B as at pH 6.0 a broad endotherm is observed with a maximum at 40–45 °C for both fragments.

Electrostatic interactions are clearly an important consideration in TM structure given the observed dependence of T_m on pH and salt concentration. These effects can best be interpreted in terms of the model of McLachlan & Stewart (1975), which is an elaboration of the proposals of Hodges et al. (1973) and Sodek et al. (1978) given the sequence (Stone et al., 1974). This model considers interchain electrostatic and hydrophobic interactions; apolar amino acids are present in the interface between the chains (positions a and d), giving rise to a large hydrophobic effect, and charge interactions act across the groove between the two chains (positions e and g). Because of the excess negative charge at neutral pH (pI = 4.6), a general increase in stability is expected if this electrostatic free energy is decreased by lowering the pH or increasing the salt concentration.

Specific electrostatic effects are suggested by the observed difference in the pH dependence of the T_m for the transitions in the TM derivatives and fragments. The transition at 41 °C in NEMTM and one of the two superimposed components at 52 °C in XLTM clearly involve a conformational change in the vicinity of Cys-190. The T_m of the component at 52 °C has a large pH dependence at pH values less than 7. This is consistent with a localized region of negative charge which increases the pK_a of carboxyl groups by the usual electrostatic work. When the disulfide link is broken, this electrostatic effect can be reduced by disordering the coiled-coil structure in this region. Thus, in the same pH range, the pH dependence of the 41 °C transition of NEMTM in this same region will be decreased as was observed. Consistent with this explanation is the fact that residues 173–196 contain the largest excess of negative charge in the TM structure (11 negative and 3 positive). The large pH dependence of the pretransition of XLTM in this same pH range suggests that this transition also occurs in a region of excess negative charge; the vicinity of Cys-190 has been suggested (Lehrer, 1978). As noted by Lehrer, this region is destabilized by formation of the disulfide link to the point that a small local conformational adjustment (the pretransition) occurs at low temperature.

The effect of breaking the disulfide link is therefore 2-fold: First, the coiled-coil structure opens slightly to reduce unfavorable electrostatic free energy in NETM, thereby precluding any local pretransition such as that observed for XLTM; Second, this disordering in NEMTM decreases the interchain interactions so that the T_m of the major transition in the vicinity of Cys-190 is markedly reduced (from 52 to 41 °C).

A second region of TM with a significant excess of negative charge is residues 54–64 (5 negative, 1 positive). The endotherms with a T_m of ~50 °C for NETM and XLTM (one of two components) have been assigned from studies of the CN1A fragment to the NH_2-terminal portion of TM which includes these residues. The pH dependence of the T_m values for this endotherm is consistent with this transition being located in a region of excess negative charge.

Electrostatic and hydrophobic interactions are the primary stabilizing forces between chains in tropomyosin, and hydrogen bonds are clearly important within the α-helical structure. The observed net heat effect for the unfolding of any protein arises from the endothermic effect of breaking these interactions compensated by the exothermic effects of the interactions of the newly exposed groups with the solvent (Privalov & Khechinashvili, 1974). For tropomyosin, the observed enthalpy for the unfolding process is ~4 cal g^{-1}, which is on the low end of the range, 4–10 cal g^{-1}, observed for the globular proteins. This likely results from the smaller number of hydrophobic contacts in a coiled-coil structure as compared to a globular protein. The observed increase in enthalpy as the T_m increases indicates that ΔC_p is positive. Globular proteins also show a positive ΔC_p, and Privalov & Khechinashvili (1974) have suggested that this enthalpy increase arises from a decrease in the ability of the amino acid side chains to form compensating interactions with the solvent as the temperature increases. A similar mechanism is appropriate to explain the observed temperature dependence of ΔH_d for tropomyosin.

The dependence of the T_m of the major endotherms on divalent cation concentration is nonlinear, and the onset of increased stability occurs at a concentration which is 100-fold smaller than is required for significant stabilization by salt. This implies a specific interaction between these metal ions and tropomyosin. This notion is supported by preliminary equilibrium dialysis experiments at pH 7.0 in 1 M KCl which indicate that Mg^{2+} binding is weak (K_a ~10^3) and saturable. Although the binding would be stronger at lower KCl concentration, the experiments were done at 1 M KCl to assure that tropomyosin was monomeric and that Donnan effects were minimized. It is our contention that divalent cations bind to the highly localized regions of negative charge and stabilize the structure by reducing unfavorable electrostatic free energy in these regions. This effect may play a role in the interactions of tropomyosin with actin as Eaton et al. (1975) have shown that tropomyosin–actin binding improves substantially as Mg^{2+} concentration is raised from 1 to 5 mM.

The unfolding of tropomyosin is clearly a multistep process. The assignment of observed endotherms to transitions in specific regions of the molecule gives an "ordering" to the unfolding in the context of the McLachlan & Stewart (1975) model. It is our intent to use these assigned transitions as probes to localize the interaction of other components of the contractile system with tropomyosin.

References

Eaton, B. L., Kominz, D. R., & Eisenberg, E. (1975) *Biochemistry 14*, 2718.

Edwards, B. F. P., & Sykes, B. D. (1980) *Biochemistry 19*, 2577.

Fernandez Diez, M. J., Osuga, D. T., & Feeney, R. E. (1964) *Arch. Biochem. Biophys. 107*, 449.

Greaser, M. L., & Gergely, J. (1971) *J. Biol. Chem. 246*, 4226.

Hartshorne, D. J., & Mueller, H. (1969) *Biochim. Biophys. Acta 175*, 301.

Hodges, R. S., Sodek, J., Smillie, L. B., & Jurasek, L. (1973) *Cold Spring Harbor Symp. Quant. Biol. 37*, 299.

Jackson, W. M. (1970) Ph.D. Thesis, University of Massachusetts.

Jackson, W. M., & Brandts, J. F. (1970) *Biochemistry 9*, 2294.

Johnson, P., & Smillie, L. B. (1975) *Biochem. Biophys. Res. Commun. 64*, 1316.

Krishnan, K. S., Brandts, J. F., & Lehrer, S. S. (1978) *FEBS Lett. 91*, 206.

Lehrer, S. S. (1975) *Proc. Natl. Acad. Sci. U.S.A. 72*, 3377.

Lehrer, S. S. (1978) *J. Mol. Biol. 118*, 209.

Mak, A. S., Lewis, W. G., & Smillie, L. B. (1979) *FEBS Lett. 105*, 232.

McLachlan, A. D., & Stewart, M. (1975) *J. Mol. Biol. 98*, 293.

Pato, M. D., & Smillie, L. B. (1978) *FEBS Lett. 87*, 95.

Potekhin, S. A., & Privalov, P. L. (1978) *Biofizika 23*, 219.
Privalov, P. L., & Khechinashvili, N. N. (1974) *J. Mol. Biol. 86*, 665.
Sodek, J., Hodges, R. S., & Smillie, L. B. (1978) *J. Biol. Chem. 253*, 1129.
Spudich, J. A., & Watt, S. (1971) *J. Biol. Chem. 246*, 4866.
Stone, D., & Smillie, L. B. (1978) *J. Biol. Chem. 253*, 1137.
Stone, D., Sodek, J., Johnson, P., & Smillie, L. B. (1974) *Proc. FEBS Meet. 31*, 125.
Woods, E. F. (1967) *J. Biol. Chem. 242*, 2859.
Woods, E. F. (1969) *Int. J. Protein Res. 1*, 29.
Woods, E. F. (1976) *Aust. J. Biol. Sci. 29*, 405.

Measurement of Medium Lysyl Oxidase Activity in Aorta Smooth Muscle Cells. Effects of Multiple Medium Changes and Inhibition of Protein Synthesis†

W. A. Gonnerman,* R. Ferrera, and C. Franzblau

ABSTRACT: Cultures of rabbit aortic smooth muscle (RSM) cells are a valuable model system for studying production and metabolism of connective tissue components. This report describes various assay procedures for lysyl oxidase, the enzyme responsible for deaminating lysine residues to give aldehyde cross-link precursors, in culture medium from these cells. Studies of the medium enzyme from second-passage RSM cells indicate that approximately 40% of the total enzyme activity in the flask of cells is in the medium. The medium enzyme levels are replenished quite rapidly following refeeding, and enzyme levels in the medium appear to be feedback controlled. The mechanism for this control is unknown at present. Multiple refeeding experiments in which the medium was changed every 2–4 h for up to 40 h indicate that these cells are capable of producing large amounts of enzyme and are capable of altering enzyme production and secretion quite rapidly in response to changes in their environment. Protein synthesis inhibitor studies with cycloheximide suggest that the major portion of the enzyme released into the medium following refeeding is newly synthesized although a pool of latent enzyme is also present. As in intact tissue, extraction of the enzyme from the cell layer requires strong denaturing reagents such as 4 M urea. These results suggest that the production of lysyl oxidase is closely regulated and is very responsive to changes in the external environment of the cells. This cell culture system appears to be an excellent one to study the production of lysyl oxidase and its role in connective tissue fibrillogenesis.

Lysyl oxidase (LO), the enzyme responsible for the oxidative deamination of key lysine residues in collagen and elastin prior to cross-link formation, plays a pivotal role in the formation of a stable, insoluble extracellular matrix. In general, this enzyme appears to function predominantly extracellularly and to be bound tightly to some component of the extracellular matrix in vivo (Chvapil et al., 1974). Thus, strong denaturing reagents such as urea are required to solubilize the enzyme prior to in vitro measurement of enzyme activity (Narayanan et al., 1974; Harris et al., 1974; Kagan et al., 1974; Chvapil et al., 1974). There have been few reports of measurement of lysyl oxidase activity in cell culture systems. Layman et al. (1972), studying lysyl oxidase activity in fibroblast cell cultures, have suggested that the enzyme levels are low and require concentration of the cell medium in order to recover measurable amounts of activity. Levine & Heslop (1977) demonstrated increased medium LO activity with increasing culture age in pig aortic endothelial cells. To date, however, there have been no reports on the kinetics of LO production in cell cultures.

This report describes techniques for measuring lysyl oxidase activity in small volumes of unconcentrated medium from rabbit aortic smooth muscle cells and IMR-90 lung fibroblasts. These methods permit serial measurements of enzyme activity over long periods of cell culture which allows one to monitor rapid changes in lysyl oxidase activity in the cell culture medium and, when appropriate, to measure enzyme production in the same cells under a variety of changing environmental conditions. By pulsing the cells with radioactive proline and measuring the amount of hydroxyproline formed, it is also possible to monitor collagen and elastin synthesis concomitantly. It is then possible to correlate the activity of key enzymes involved in the posttranslational processing of collagen and elastin with biosynthesis of these major connective tissue proteins and their incorporation into the extracellular matrix.

Materials and Methods

Cell Culture. Two cell types were used in this series of experiments. Cultures of IMR-90 fibroblasts, an embryonic human lung derived fibroblast strain (Nichols et al., 1977), were obtained from the Institute for Medical Research, Camden, NJ. These cells were subcultured and were used at population doubling levels (PDL) 24–28. These cells were grown in T-75 flasks with 20 mL of modified Eagle's medium (Daniel & Melendez, 1968) containing 2.2 g/L $NaHCO_3$, 10% fetal bovine serum (FBS), penicillin (100 units/mL), and streptomycin (100 μg/mL). Ascorbic acid was not included in the growth medium.

Rabbit aortic smooth muscle cells were derived from explants of the aortic arch from weanling rabbits as described previously (Faris et al., 1976). Cells were used during the

† From the Department of Biochemistry, Boston University School of Medicine, Boston, Massachusetts 02118. *Received September 19, 1980.* This work was supported in part by National Institutes of Health Grants HL 19717 and HL 13262.

0006-2960/81/0420-3864$01.25/0